Properties and Degradation Behavior of Surface Functionalized MWCNT/Poly(L-lactide-co-ε-caprolactone) Biodegradable Nanocomposites

Maryam Amirian, Jiehe Sui, Ali Nabipour Chakoli, Wei Cai

School of Material Science and Engineering, Harbin Institute of Technology, Harbin 150001, Heilongjiang Province, People's Republic of China

Received 24 March 2010; accepted 6 February 2011
DOI 10.1002/app.34317
Published online 7 July 2011 in Wiley Online Library (wileyonlinelibrary.com).

ABSTRACT: In this research, poly(L-lactide-co-ε-caprolactone) (PLACL) reinforced with well-dispersed multiwalled carbon nanotubes (MWCNTs) nanocomposites were prepared by oxidization and functionalization of the MWCNT surfaces using oligomeric L-lactide (LA) and ε-caprolactone (CL). It is found that the surface functionalization can effectively improve the dispersion and adhesion of MWCNTs in PLACL. The surface functionalization will have a significant effect on the physical, thermomechanical, and degradation properties of MWCNT/PLACL composites. The tensile modulus, yield stress, tensile strength, and elongation at break of composite increased 49%, 60%, 70%, and 94%, respectively, when the concentration of functionalized MWCNTs in composite is 2 wt %. The *in vitro* degradation rate of nanocomposites in phosphate buffer solution increased about 100%. The glass transition temperature (T_g) of composites was decreased when the concentration of functionalized MWCNTs is 0.5 wt %. With further increasing the concentration of functionalized MWCNTs, the T_g was increased. The degradation kinetics of nanocomposites can be engineered and functionalized by varying the contents of pristine or functionalized MWCNTs. © 2011 Wiley Periodicals, Inc. J Appl Polym Sci 122: 3133–3144, 2011

Key words: composites; biodegradable; functionalization; multiwalled carbon nanotubes; poly(L-lactide-co-ε-caprolactone)

INTRODUCTION

The multiwalled carbon nanotubes (MWCNTs) have attracted a great deal of interest in both science and engineering fields since they were discovered.[1] Their superior Young's modulus, high electrical conductivity, and thermal conductivity make MWCNTs highly attractive for multifunctional polymer composite applications. Furthermore, their small diameter and large aspect ratio offers additional advantages for composite applications. In the past few years, MWCNTs have been incorporated into a wide range of polymer matrices for various functional applications.[2–5]

However, to fully impart the high strength of MWCNTs to polymers, significant efforts are still needed to overcome poor dispersion and poor adhesion of MWCNTs to the polymer matrices. Because of the intrinsic Van der Waals force attraction and high aspect ratio nature, MWCNTs are usually present in the form of bundles and ropes. Consequently, dispersion of MWCNTs in a media becomes a challenge. When the MWCNTs are mixed with polymers, they will usually aggregate in polymer matrices. The poor dispersion of MWCNTs not only significantly lowers their efficiency as a reinforcement but also cause MWCNTs to slip by each other when forces are applied to the composites. To apply the full potential ability of pristine MWCNTs (pMWCNT)s as reinforcing fillers for polymers, there are two important key points: (1) homogenous dispersion of individual MWCNTs in polymer matrix and (2) efficient adhesion between the sidewall of pMWCNTs and polymer matrix. The low adhesive effect between the MWCNTs and polymer matrix causes the agglomeration and entanglement of pMWCNTs together because of intrinsic Van der Waals force attraction between pMWCNTs.[6,7]

Biodegradable, biocompatible, and shape memory polymers such as poly(L-lactide) PLLA, poly(ε-caprolactone) (PCL), and their copolymer (PLACL) have been widely studied for various pharmaceutical and medical applications, such as surgical sutures, tissue engineering, and controlled drug delivery systems. PLLA is a thermoplastic polyester with high strength and high modulus that can be produced from renewable sources. It can be easily processed to yield articles to be used in the industrial packaging and biocompatible and bioabsorbable field such as

Correspondence to: J. Sui (suijiehe@hit.edu.cn).
Contract grant sponsor: Excellent Youth Foundation of Heilongjiang Province of China; contract grant number: JC200715.

drug delivery systems and in applications for sutures and surgical implants. The PLLA is hardly permeable to most drugs, and its degradation rate is high. Among them, PCL is permeable to many drugs, but its degradation rate is very low. Thus, the copolymerization of ε-caprolactone (CL) and L-lactide (LA) is an effective strategy of combining the great permeability of PCL and the rapid biodegradation of PLLA component. Of these polymers, PLACL is a commonly used polymer that has significant potential in the manufacture of degradable vascular structures and cartilages. Compared with most other biodegradable plastics, PLACL is a thermoplastic elastomer that has high elongation, moderate tensile strength, and Young's modulus. More notably, it is reported that PLACL is a shape memory polymer. Degradable shape memory polymer is of great importance in medical applications.[8–13]

However, these polymers lacked sufficient mechanical properties for medical applications such as hard tissue engineering. To achieve the earlier goal, various fillers, such as bioglass,[14] biphasic calcium phosphate,[15] hydroxyapatite,[16] Kenaf fibers,[17] and CNTs,[18] have been added to the PLLA and PLACL as the reinforcement. Wu et al.[19–21] prepared PLLA and PCL composites containing pristine, carboxylated, and hydroxylated MWCNTs directly by melt compounding. In their next research, they used carboxylated MWCNTs to control the morphology of immiscible PCL/PLLA blend. Jana and Cho grafted PCL-diol onto the surface of acylchloride-functionalized MWCNTs (MWCNT-COCl) by grafting to approach to form PCL-graft-MWCNTs.[22,23] Kim et al.[24] grafted PLLA onto the surface of hydroxylated MWCNTs and prepared the composite of PLLA with PLLA-grafted MWCNTs by melt compounding. Saeed et al.[25,26] at first functionalized MWCNTs by Friedele–Crafts acylation, which introduced the aromatic amine groups on the sidewall of prepared MWCNT composite by *in situ* polymerization using functionalized MWCNTs. In their next research, they grafted PCL on to the pristine and carboxylated MWCNTs. Chen and Shimizu[27] functionalized MWCNT-COCL with polyhedral oligomeric silsesquioxane via amide linkages. Zeng et al.[28] grafted PCL onto the surface of hydroxylated MWCNTs and studied the enzymatic degradation of grafted PCL on MWCNTs. In our last research, we successfully deposited monodisperse magnetite nanoparticles with sizes <10 nm on MWCNTs by *in situ* high-temperature decomposition of the precursor iron(III) acetylacetonate and MWCNTs in polyol solution and then grafted PLLA from the sidewall of the prepared magnetic MWCNTs. In our previous research, we synthesized PLACL grafted from the sidewall of MWCNTs (MWCNT-*g*-PLACL) and studied the morphology of grafted polymer on the sidewall of MWCNTs.[29–31]

In this article, the effects of pMWCNT dispersion and surface treatment on the mechanical and degradation properties of MWCNT-reinforced PLACL composites are reported to understand their structure property relationship. The effect of pristine MWCNTs and PLACL grafted from MWCNTs on *in vitro* degradation of PLACL was investigated.

EXPERIMENTAL

Materials

Pristine MWCNTs (pMWCNTs) were purchased from the Nanotech Port Company (Shenzhen, China). The diameter of MWCNTs is 5–20 nm, length is 5–15 μm, and the specific surface area is 40–300 $m^2\ g^{-1}$. The L-lactic acid (PURAC Biochem, Spain) was used as received. Stannous octanoate [$St(Oct)_2$] (Shanghai chemical reagent company, China) was used as a catalyst. Chloroform, methanol, toluene, tetrahydrofuran (THF), thionyl chloride ($SOCl_2$), and ethylene glycol were purchased from Kermel of China as analytic reagent. The CL (Acros, Belgium) was stored in the presence of 4–6 Å molecular sieves before use to eliminate traces of water. The phosphate buffer solution (PBS) (Boster Bio-Technology Company, China), which contains 0.02*M* phosphate and 0.15*M* NaCl, was solved in 2 L of deionized water.

Functionalization of MWCNTs

The pMWCNTs were first oxidized by a mixture of sulfuric acid and nitric acid. Then the oxidized MWCNTs were reacted with $SOCl_2$. The prepared solid was reacted with ethylene glycol for 48 h at 120°C. The hydroxylated MWCNTs (MWCNT-OHs) were separated, washed with THF, and dried in oven at 50°C. The LA and CL comonomers were added into a flask with $Sn(Oct)_2$ as initiator and MWCNT-OHs as coinitiator and then heated at 130°C for 48 h. The synthesized material was purified using chloroform. The details of functionalization and characterization of MWCNTs were presented in our last publication.[29]

Preparation of composites

The MWCNT-*g*-PLACLs, which were dispersed in chloroform with various concentrations, were mixed with neat PLACL80 (80 wt % LA + 20 wt % CL) in chloroform to achieve MWCNT-*g*-PLACL/PLACL80 composites having 0.5, 1.0, 2.0, and 3.0 wt % loading of MWCNT-*g*-PLACLs. The LA oligomer and PLACL copolymers were prepared as introduced in our previous work.[29] The mixtures were left in glass molds two days at room temperature for chloroform

evaporation, and then the glass molds containing composite films were dried in an oven at 45°C for 2 days to completely evaporation of solvent. The composites film were removed from glass molds and cut for characterization. For comparison purposes, a neat PLACL80 sample and pMWCNT/PLACL80 composites of 0.5, 1.0, 2.0, and 3.0 wt % loading of pMWCNTs were also prepared.

Characterization

The FTIR spectra of pristine and functionalized MWCNTs were recorded between 500 and 4000 cm^{-1} using a Perkin–Elmer Spectrum One FTIR (MA) spectrometer. A minimum of 16 scans were averaged with a signal resolution of 4 cm^{-1} within the 500–4000 cm^{-1} range. Scanning electron microscope (SEM) images of MWCNTs and the fracture surfaces of the composites were acquired using a Hitachi *S*-4700 field-emission system (Tokyo, Japan). The fracture surface of tensile test samples after breaking was sputter coated with a thin layer (~ 3 nm) of Au prior to SEM imaging. The X-ray diffraction (XRD) method was employed for studying the crystalline structure by using a Rigaku D/max-rb rotating anode X-ray diffractometer (TX) at 50 kV and 40 mA (CuKα, $\lambda = 1.5406$ Å). The thermal properties of prepared materials were investigated using a simultaneous thermal analyzer model ZRY-2P (Shanghai Balance Co, China) by scanning from 30 to 600°C at heating rate of 20°C/min under nitrogen atmosphere. The differential scanning calorimetry (DSC) was carried out with a Perkin–Elmer Diamond DSC (MA). Samples (10 ± 0.5 mg) were placed in aluminum crucibles. An empty aluminum crucible was used as reference. Samples were heated from −30 to 200°C under nitrogen flow and heating rate of 20°C/min.

Mechanical testing

Tensile properties of PLACL composites were obtained based on ASTM D638 method. The tensile tests were performed using a microcontroller electronic tension meter model WDW3100 (Guangzhou Jing Mi, China) machine at a crosshead speed of 5.0 mm/min at ambient temperature. Young's modulus, tensile strength, and elongation at break of each sample were obtained based on at least three specimens per sample.

Dynamic mechanical analysis (DMA) was conducted for thermomechanical characterization using a Q800 dynamic mechanical analyzer (TA Instruments, New Castle, DE) under tension mode, ranging from −20 to 100°C, at a fixed frequency of 1 Hz and with a temperature increment of 20°C/min. The maximum point on the tan δ curve was chosen as the glass transition temperature (T_g) of the samples.

In vitro degradation test

The neat PLACL80 and its composite with both kinds of fillers were hydrolyzed in a time interval of 0−12 weeks in 50-mL PBS at pH 7.4, within a thermostatically controlled bath at 37°C (i.e., approximate human body conditions reproduced *in vitro*). The pH was kept constant by replacing the buffer solution weekly with a fresh one. After predetermined intervals of time, the samples were taken out, washed with distilled water, and dried in oven at 45°C for 2 days to extract the maximum possible amount of water until a constant weight was obtained. Then, the weight loss was calculated for each sample. Degradation of MWCNT-*g*-PLACL was performed by immersion of 50 mg of MWCNT-*g*-PLACLs in 50-mL PBS at pH 7.4 at 37°C for 12 weeks. The degraded MWCNT-*g*-PLACLs were washed with high pure water and dried in oven at 45°C over night then washed with chloroform to remove excess ungrafted polymer and dried in oven at 45°C over night.

RESULTS AND DISCUSSION

Structural characterization

Figure 1 gives the FTIR spectra of acid-modified MWCNTs, primary MWCNT-*g*-PLACLs, neat PLACL60, and *in vitro* degraded MWCNT-*g*-PLACLs. Carboxylic group stretching (COOH) appears at 1715 cm^{-1}, which corresponds to the incorporated carboxylic acid groups as a result of acid treatment and carboxylation. The large FTIR band observed at 3420 cm^{-1} is attributed to the

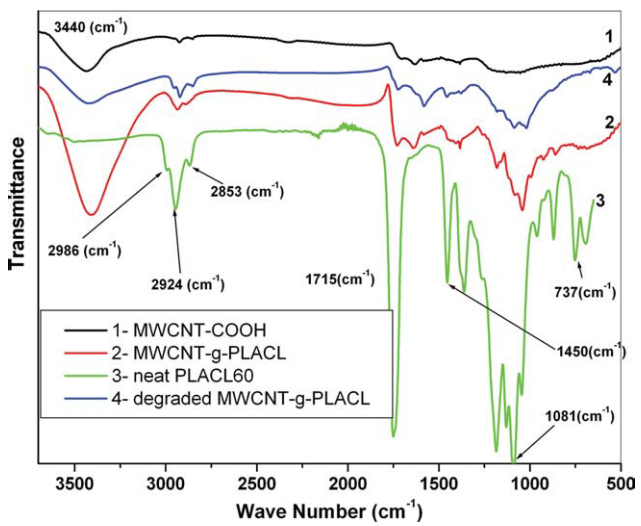

Figure 1 The FTIR spectra of carboxylated MWCNTs (1), primary MWCNT-*g*-PLACLs (2), neat PLACL60 (3), and *in vitro* degraded MWCNT-*g*-PLACLs in PBS at 37°C and pH 7.4 after 3 months(4). [Color figure can be viewed in the online issue, which is available at wileyonlinelibrary.com.]

absorption peak of —OH that arise from trace amounts of water [Fig. 1(1)]. In Figure 1(2), the feature at 3450–3400 cm^{-1} corresponds to the absorption of —OH stretching of hydroxyl groups. Peaks at 2986, 2924, and 2853 cm^{-1} correspond to $—CH_3$ absorption and the $—CH_2$ absorption band that refereed to LA and CL of grafted PLACL chains on the sidewall of MWCNTs. The feature at 1770–1710 cm^{-1} corresponds to the absorption band of C=O stretching vibration that belongs to carbonyl groups of grafted PLACL. The C—O stretching vibrations of asymmetrical coupled vibration of C—CO—O refereed to both of LA and CL. These vibrations are at 1088 and 1183 cm^{-1}. The resonances due to $C—CH_3$ stretching mode, $—CH_3$ rocking mode, and $—CH_3$ asymmetric bending mode of LA part of PLACL are at 1047, 1127, and 1450 cm^{-1}, respectively. The resonance due to CH_2 rocking mode of CL, part of PLACL in Figure 1(2), is at 862 and 737 cm^{-1}. Figure 1(3) shows the FTIR spectra of neat PLACL60. As a comparison between Figure 1(2,3), it confirms that the PLACL chains have successfully grafted from the sidewall of MWCNTs. After *in vitro* degradation of MWCNT-*g*-PLACLs, the peaks refereed to the grafted PLACL chains were significantly decreased or disappeared, especially the resonance due to $—CH_2$ rocking mode of CL part of PLACL is at 862 and 737 cm^{-1}, because of full degradation of CL from the surface of MWCNTs [Fig. 1(4)]. The —OH stretching absorption peak of hydroxyl groups and C—O stretching vibrations of asymmetrical coupled vibration of C—CO—O refer to both of LA and CL at 1088 and 1183 cm^{-1} were significantly decreased.

Figure 2 compares the thermal degradation of carboxylated MWCNTs with primary MWCNT-*g*-PLACLs and degraded MWCNT-*g*-PLACLs. It can be found that the 20 wt % of an individual MWCNT-*g*-PLACL refers to MWCNT, and the 80 wt % of it refers to the grafted materials.[30] The thermal degradation analysis shows that the degraded MWCNT-*g*-PLACLs have a 20 wt % weight loss until 500°C, while the primary MWCNT-*g*-PLACLs have 80 wt % weight loss and the carboxylated MWCNTs have 13 wt % weight loss until 500°C. Hence, the 7 wt % of degraded MWCNT-*g*-PLACLs is refereed to the grafted polyethylene glycol and carboxyl groups remained on the surface of MWCNTs after *in vitro* degradation. The results show that the grafted-PLACL chains on the sidewall of MWCNTs were degraded in PBS.

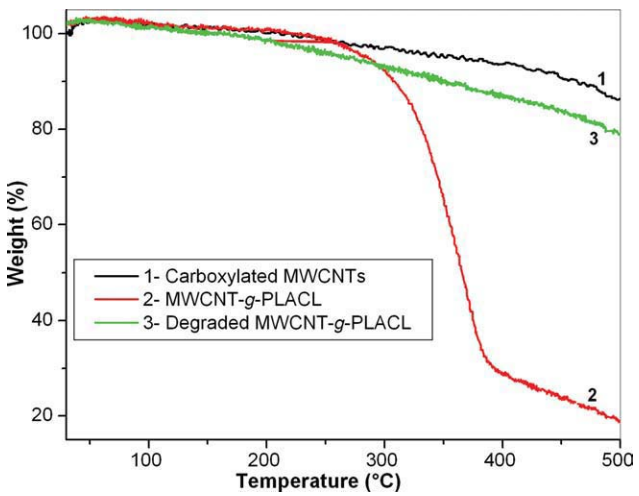

Figure 2 The thermal degradation results of carboxylated MWCNTs (1), PLACL-grafted MWCNTs (2), and *in vitro* degraded PLACL-grafted MWCNTs in PBS at 37°C and pH 7.4 after 3 months (3). [Color figure can be viewed in the online issue, which is available at wileyonlinelibrary.com.]

Morphology characterization

The morphology of MWCNT-*g*-PLACLs before and after degradation was characterized using SEM. Figure 3(a) shows the surface morphology of hydroxylated MWCNTs that used for grafting of PLACL chains from the surface of MWCNTs. They are shortened, individual, and did not entangle to each other. The SEM micrographs in Figure 3(b) show the MWCNT-*g*-PLACLs are entangled to each other because of grafted polymer chains. The grafted polymer chains of MWCNT-*g*-PLACLs are entangled to each other like hair brushes. It is found that the entanglement of grafted polymers disappeared on the surface of degraded MWCNT-*g*-PLACLs, as can be seen in Figure 3(c), due to fully degradation of grafted PLACL chains.

Crystallinity of neat PLACL80 and its composites

The XRD pattern of the neat PLACL80 and its composites with pMWCNTs and MWCNT-*g*-PLACLs are shown in Figure 4. As can be seen, the pattern shows there are three significant diffraction peaks at 16.9° (peak 1), 19.2°(peak 2), and 22.5° (peak 3), which characterize the crystalline phase of PLACL80, reveal typical of α-form described as pseudo-orthorhombic, pseudohexagonal, or orthorhombic.[31,32] It is found that both of pMWCNTs and MWCNT-*g*-PLACLs as heterogeneous nucleation point increased the crystallinity of PLACL80 when the contents of fillers were increased until 2 wt %. The crystallinity of composites had no significant change with increment of filler contents from 2 to 3 wt %. The decreasing of full width at half maximum (FWHM) is related to increasing the lamellae size of crystalline phase. The effect of MWCNT-*g*-PLACLs on the crystallinity of composites is more regular than pMWCNTs.

Both kinds of MWCNTs at the concentration of 0.5 wt % decrease the melting point of composites;

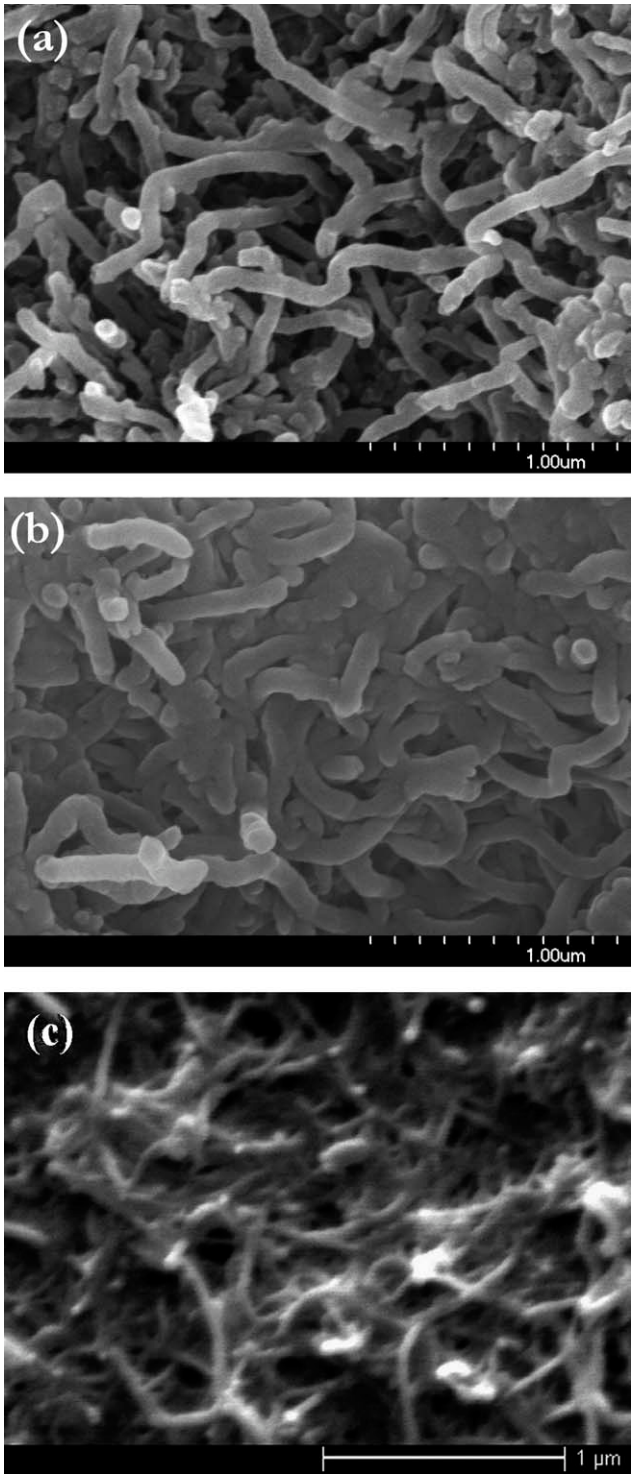

Figure 3 The SEM micrograph of hydroxylated MWCNTs (a), PLACL grafted from the MWCNTs (b), and the degraded of PLACL chains grafted from the sidewall of MWCNTs in PBS at 37°C and pH 7.4 for 3 months (c).

however, at the concentration of more than 1 wt %, pMWCNTs increase the melting point of composite, and the MWCNT-*g*-PLACLs has no significant effect on the melting point (Table I). It is due to the unity of grafted polymer chains on the sidewall of MWCNTs and polymer matrix. The melting enthalpy of MWCNT-*g*-PLACL/PLACL80 are increased with increasing the concentration of MWCNT-*g*-PLACLs. Therefore, the crystallinity of composites are increased with increasing of the concentration of MWCNT-*g*-PLACLs. The pMWCNTs have the same effect on composites, while the increment of melting enthalpy of pMWCNT/PLACL80 is less than that of MWCNT-*g*-PLACL/PLACL80.

Dynamic mechanical behavior

Temperature-dependent mechanical properties were characterized by DMA at a ramp rate of 20°C/min, 1 Hz. Typical DMA curves are shown in Figure 5. The storage modulus indicates the amount of energy stored in the composite as elastic energy, which is highly affected by the filler mechanical properties and geometric characteristics, the interfacial bonding between filler and matrix, and the filler loading [Fig. 5(a,b)]. The ratio of loss modulus to storage modulus

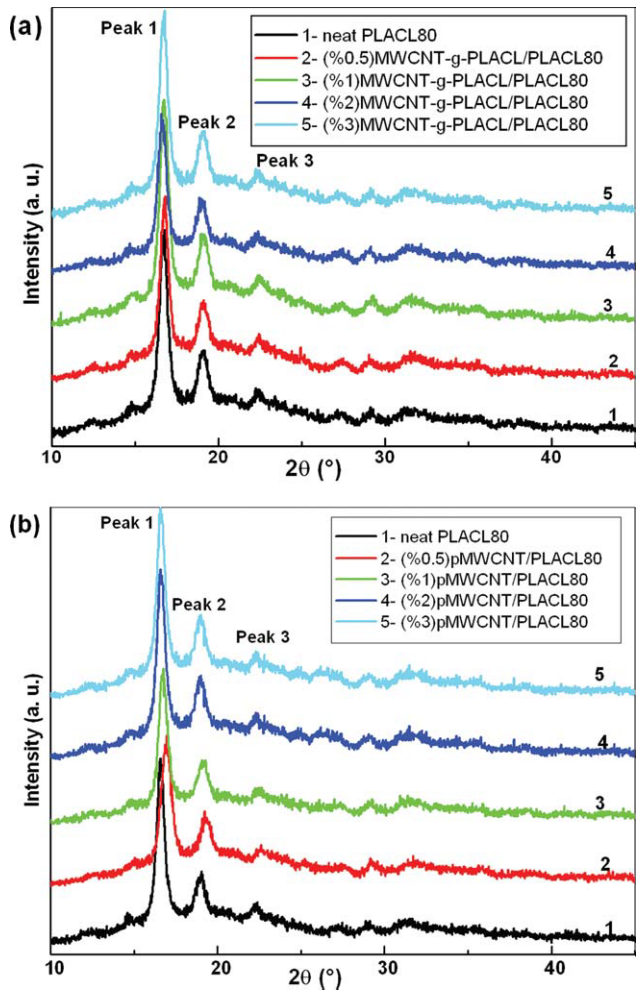

Figure 4 X-ray diffraction patterns of neat PLACL80 and its composites with various amounts of MWCNT-*g*-PLACLs (a) and pMWCNTs (b). [Color figure can be viewed in the online issue, which is available at wileyonlinelibrary.com.]

TABLE I
Melting Temperature (T_m) and Melting Enthalpy (ΔH_m) of Neat PLACL80 and Its Composites with Various Concentrations of MWCNT-*g*-PLACL and pMWCNTs

Filler contents (wt %)	MWCNT-*g*-PLACL/PLACL80		pMWCNT/PLACL80	
	Tm (°C)	ΔH_m (J/g)	T_m (°C)	ΔH_m (J/g)
0	162.3	27.6	162.3	27.6
0.5	161.5	27.8	160.2	27.9
1	162.1	29.4	163.5	28.4
2	162.5	29.9	165.9	28.9
3	162.6	30.2	167.9	29.2

is called tan δ (tan delta), whose peak is a suggestion of a glass transition [Fig. 5(c,d)]. Both kinds of fillers demonstrated a significant increase in the storage modulus compared with neat PLACL80. Moreover, the T_g of the composite has significantly decreased when the concentration of fillers was 0.5 wt % and then increased with further increasing of fillers in composite. However, the maximum T_g of composites is less than that of neat PLACL80. Owing to the same dimension scale, both kinds of MWCNTs interfere with the crystallization behavior of the PLACL80. The T_g of neat PLACL80 is about 59°C, it is 54.7°C for (3 wt %) pMWCNT/PLACL80 and 53.7°C for the MWCNT-*g*-PLACL/PLACL80. The T_g of pMWCNT/PLACL80 is higher than that of MWCNT-*g*-PLACL/PLACL80 with the same amount of fillers. It is found that MWCNT-*g*-PLACL/PLACL80 is slightly softer than pMWCNT/PLACL80.

Obviously, the significant increase of storage modulus resulted from improved interfacial bonding between the MWCNT and polymer matrix, since the PLACL groups grafted onto the MWCNT reacted with the polymer chains of matrix during casting. The integrated MWCNTs efficiently improved the load transfer and then enhanced the reinforcement effect. The consistent results DMA characterizations

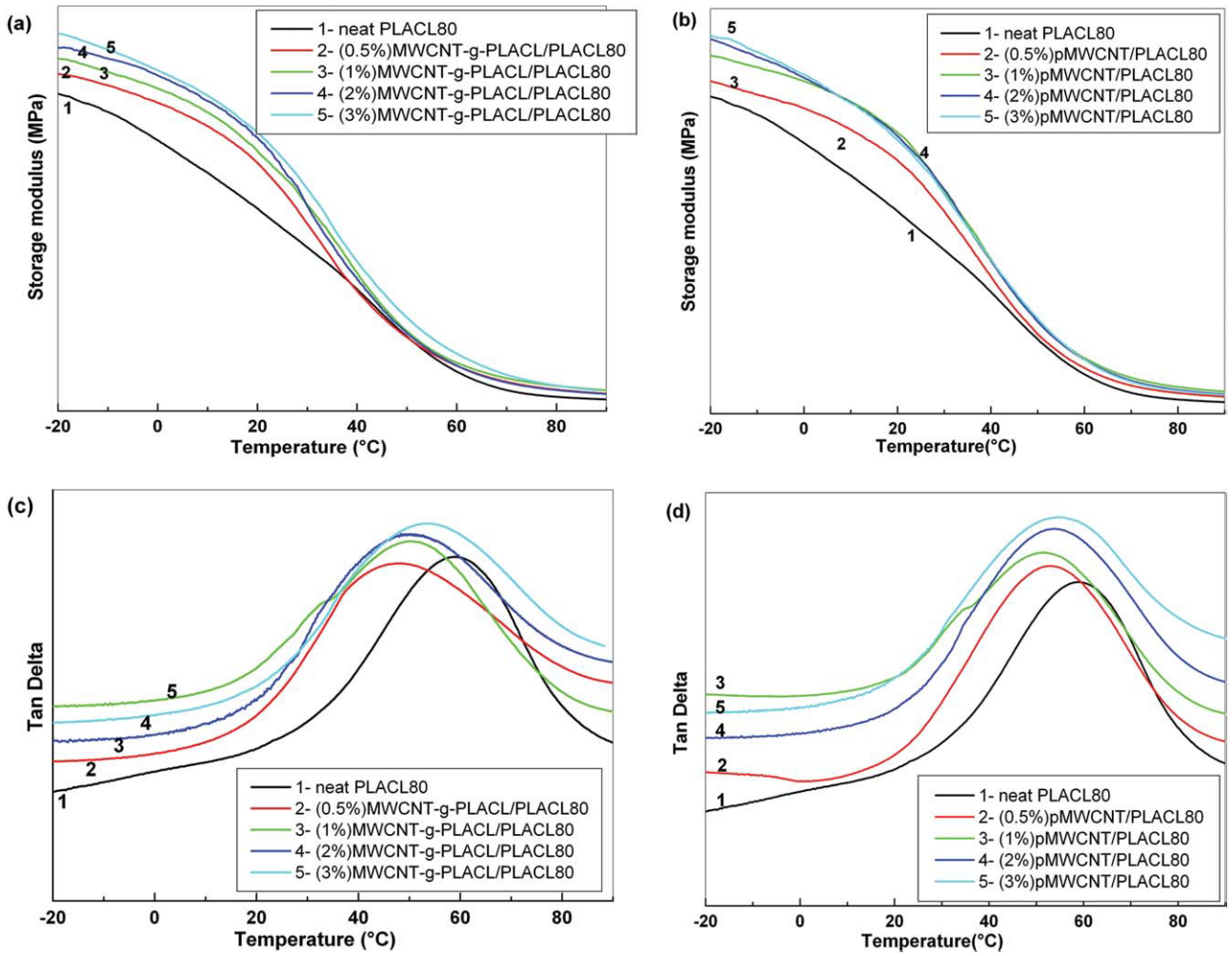

Figure 5 DMA results of neat PLACL and its composites with various amounts of fillers. Storage modulus and tan delta of MWCNT-*g*-PLACL/PLACL80 (a,c) and storage modulus and tan delta of pMWCNT/PLACL80 (b,d). [Color figure can be viewed in the online issue, which is available at wileyonlinelibrary.com.]

TABLE II
Tensile Test Results of PLACL80 and Its Composite with Various Concentrations of MWCNT-*g*-PLACL and pMWCNT as Reinforcing Fillers

	MWCNT-*g*-PLACL/PLACL80				pMWCNT/PLACL80			
Filler contents (wt %)	Tensile modulus (GPa)	Yield stress (MPa)	Tensile strength (MPa)	Elongation at break (%)	Tensile modulus (MPa)	Yield stress (MPa)	Tensile strength (MPa)	Elongation at break (%)
0	1.05	16	23.6	257	1.05	16.0	23.6	257
0.5	1.26	20.2	27.2	343	1.30	17.7	21.8	244
1	1.47	21.6	29.9	378	1.34	18.9	24.4	236
2	1.56	24.3	44.8	491	1.35	20.0	24.7	235
3	1.48	25.9	39.3	499	1.37	22.1	26.7	197

indirectly validated the existence of the PLACL groups on the nanotube surface after covalent functionalization.

Tensile and fracture behavior

The tensile test results are summarized in Table II. The results show that the incorporation of pMWCNTs can improve the PLACL80 tensile modulus, yield stress, and tensile strength but decrease the elongation at failure. The incorporation of MWCNT-*g*-PLACLs leads to the best overall reinforcing effect in tensile modulus, yield stress, tensile strength, and elongation at failure.

The SEM micrographs in Figure 6 are refereed to the surface of MWCNT-*g*-PLACL/PLACL80 and pMWCNT/PLACL80 composites elucidate that the most of pMWCNTs are entangled to each other. It can be seen that the entanglements of MWCNT-*g*-PLACLs in composites are significantly less than that of pMWCNTs in composites. The most of entangled points in pMWCNT/PLACL80 are connected to each other by pMWCNTs. This effect is because of the length of pMWCNTs and incorporation of pMWCNTs into the entangled points. The SEM image refers to the fracture surface of pMWCNT/PLACL80 after tensile test [Fig. 7(a,b)], showing that the pMWCNTs are agglomerated and the adhesion between pMWCNTs and polymer matrix is generally poor, as many pMWCNTs are pulled out of the matrix and show no sign of polymer attached to the bare pMWCNTs. While on the fracture surface of the MWCNT-*g*-PLACL/PLACL80 [Fig. 7(c,d)], it is shown that the MWCNTs are not only well dispersed throughout the matrix but their adhesion to the PLACL80 matrix is also greatly improved since most of the MWCNT-*g*-PLACLs on the fracture surface are broken. On the basis of earlier findings, functionalization of MWCNTs can improve the dispersion and adhesion between MWCNTs and PLACL80 matrix. It is necessary to consider that the 20 wt % of an individual MWCNT-*g*-PLACL refers to MWCNT, and the 80 wt % of it refers to the grafted materials. It means that the concentration of MWCNTs in (1 wt %) MWCNT-*g*-PLACL/PLACL80 composite is 0.2 wt % of the mentioned composites. Hence, it can be found that the significant effect of grafted polymer chains on the sidewall of MWCNTs is to improve the adhesion

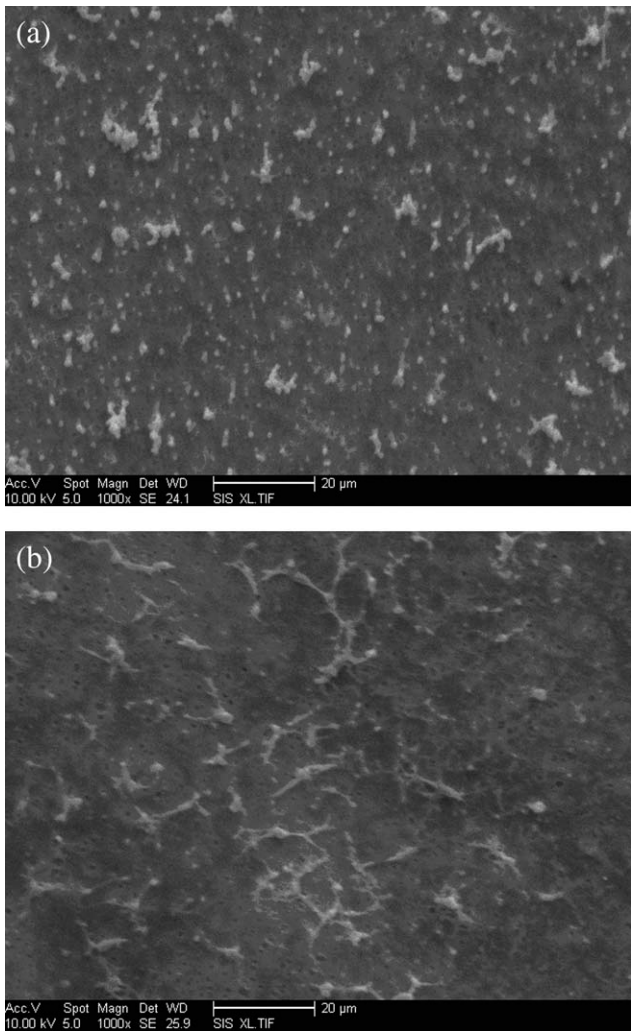

Figure 6 The SEM micrograph belong to the surface of (3 wt %) MWCNT-*g*-PLACL/PLACL80 (a) and (3 wt %) pMWCNT/PLACL80 (b) nanocomposites.

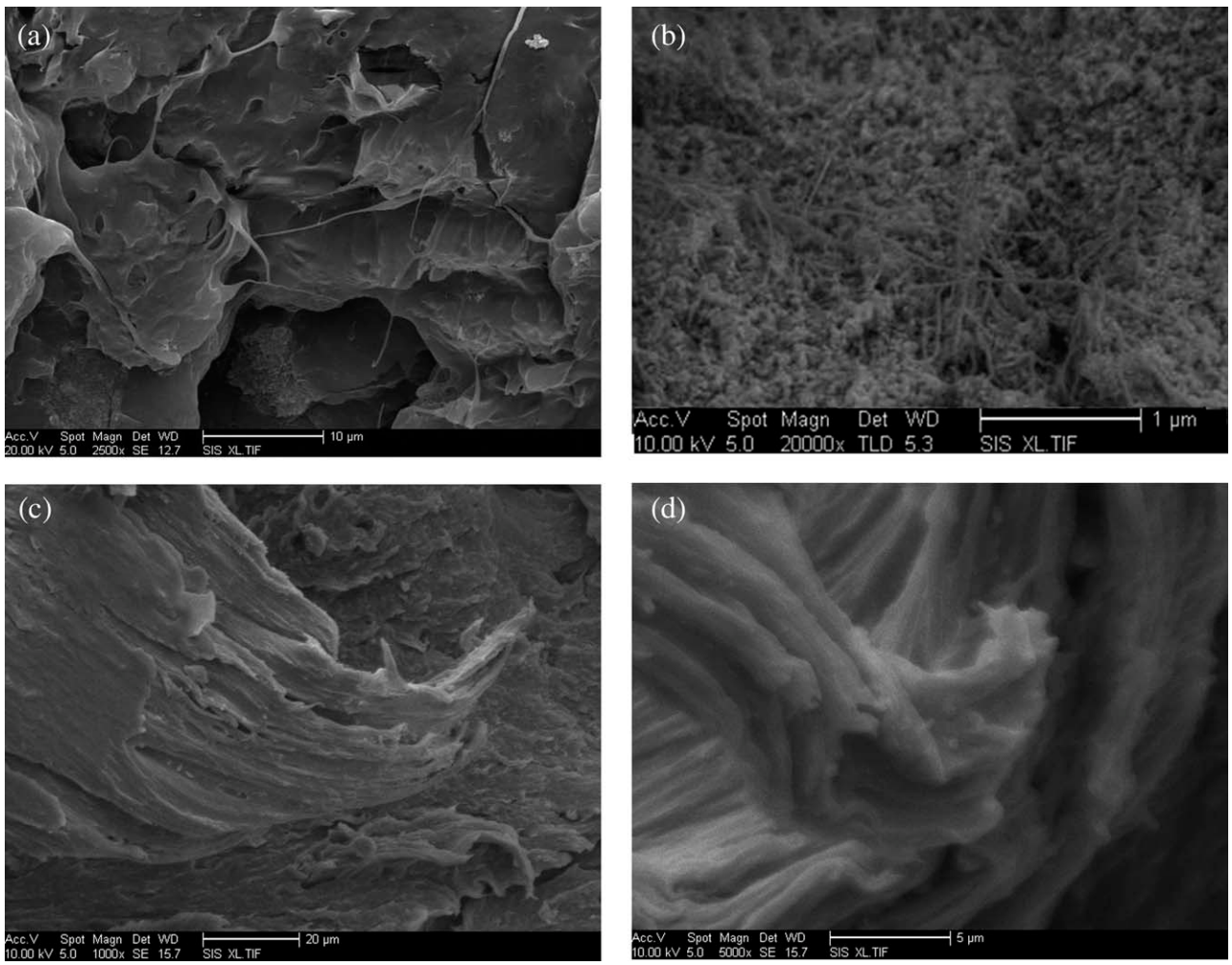

Figure 7 SEM images of fracture surface of composite samples: (a) (2 wt %) pMWCNT/PLACL80, poor dispersion, poor adhesion; (b) enlarged region from (a), (c) (2 wt %) MWCNT-*g*-PLACL80, good dispersion, good adhesion; and (d) enlarged region from (c).

effect between MWCNTs and matrix and furthermore improving the mechanical properties of composites.

In vitro degradation of neat PLACL80 and its composites with MWCNTs

The *in vitro* degradation can be divided into three steps. In the first step, the polymer takes up water and swells, but there is no mass loss. In the second step, the molecular weight decreases significantly, and the material looses its mechanical strength. The hydrolysis is autocatalyzed by carboxylic acid groups, which they are produced by the cleavage of ester bonds. In the third step, when the molecular mass falls below a critical value, mass loss sets in, and the degraded fragments diffuse into the surrounding medium.

The *in vitro* degradation of neat PLACL80 and its composites was started by surface erosion in PBS. The SEM micrographs in Figures 8 and 9 compare the surface erosion of composites that have been left in PBS for six weeks with the concentration of both kinds of MWCNTs (1 and 3 wt %). As can be seen, the surface of degraded neat PLACL80 has many cracks that were created during degradation. After creation of cracks, the PBS diffuse inside the cracked points and degrades the inside wall of crack points leading to increase the deepness of cracks. With increasing the concentration of MWCNT-*g*-PLACLs, the surface density of cracks was decreased [Fig. 8(b,c)]. All samples of neat PLACL80 and its composites with both kinds of fillers have found cracks on their surface after degradation. The density of cracks on the surface of degraded (3 wt %) MWCNT-*g*-PLACL/PLACL80 is less than that of neat PLACL80 [Fig. 8(c)]. It is because of efficient reinforcement of MWCNT-*g*-PLACLs and high interfacial interaction between MWCNTs and polymer matrix that prevent cracking during degradation. Beside the crack points on the surface of samples, the surface erosion of composites is higher than that of neat PLACL80. Both kinds of MWCNTs can increase the surface

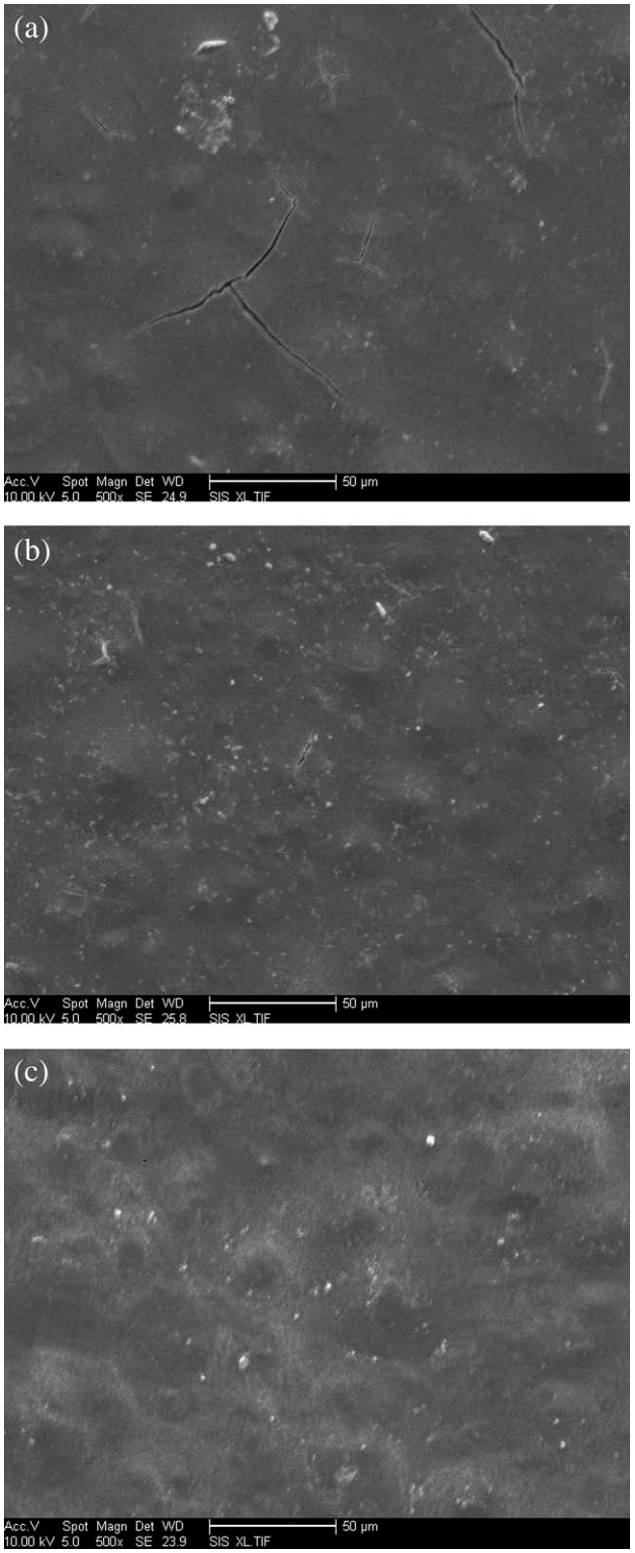

Figure 8 The surface morphology of neat PLACL80 (a), (1 wt %) MWCNT-*g*-PLACL/PLACL80 (b), and (3 wt %) MWCNT-*g*-PLACL/PLACL80 (c) after degradation in PBS at 37°C and pH 7.4.

erosion of PLACL80 in composites. Higher concentrations of pristine and the functionalized MWCNTs in the matrix have significant effect on surface erosion of composites. In pMWCNT/PLACL80 as can be seen in Figure 9, there is a lack of compatibility between pMWCNT and matrix. Hence, PBS solution can diffuse inside the bulk of matrix from this interface zone. In MWCNT-*g*-PLACLs/PLACL80 composites, the hydrolysis rate of PLACL grafted chains is higher than bulk PLACL80. Hence, the PBS solution can diffuse inside the bulk of matrix from these interface zones. However, the PBS diffusion zones on the surface of composites created by MWCNTs are smaller than cracks, but the surface density of these zones are much higher than the surface density of cracks. With increasing the concentration of MWCNTs in composites, the density of diffusion zones increased. Therefore, the degradation rate increased. It means that the pMWCNT/PLACL80 losses its mechanical strength during degradation faster than that of MWCNT-*g*-PLACL/PLACL with the same amount of fillers.

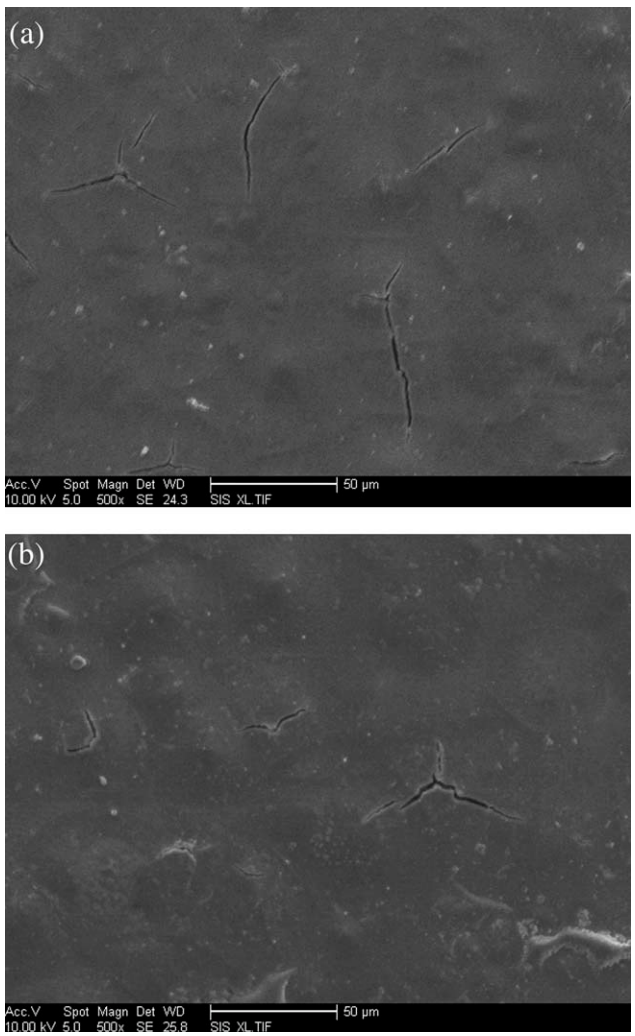

Figure 9 The surface morphology of (1 wt %) pMWCNT/PLACL80 (a) and (3 wt %) MWCNT/PLACLR80 (b) after degradation in PBS at 37°C and pH 7.4.

TABLE III
Melting Temperature (T_m) and Melting Enthalpy (ΔH_m) of Neat PLACL80 and Its Composites with Various Concentrations of MWCNT-*g*-PLACL and pMWCNTs After 6 Weeks *In Vitro* Degradation in PBS

Filler contents (wt %)	MWCNT-*g*-PLACL/PLACL80		pMWCNT/PLACL80	
	T_m (°C)	ΔH_m (J/g)	T_m (°C)	ΔH_m (J/g)
0	168	39.4	168	39.4
0.5	167	29.1	162.4	37.2
1	166.1	31	163.5	37.5
2	165.5	34.1	166.8	38.1
3	164.7	38.5	164.7	38.7

The melting temperature (T_m) and melting enthalpy (ΔH_m) of neat PLACL80 and its composites with various amounts of fillers after six weeks *in vitro* degradation in PBS are summarized in Table III. The melting point of PLACL composites

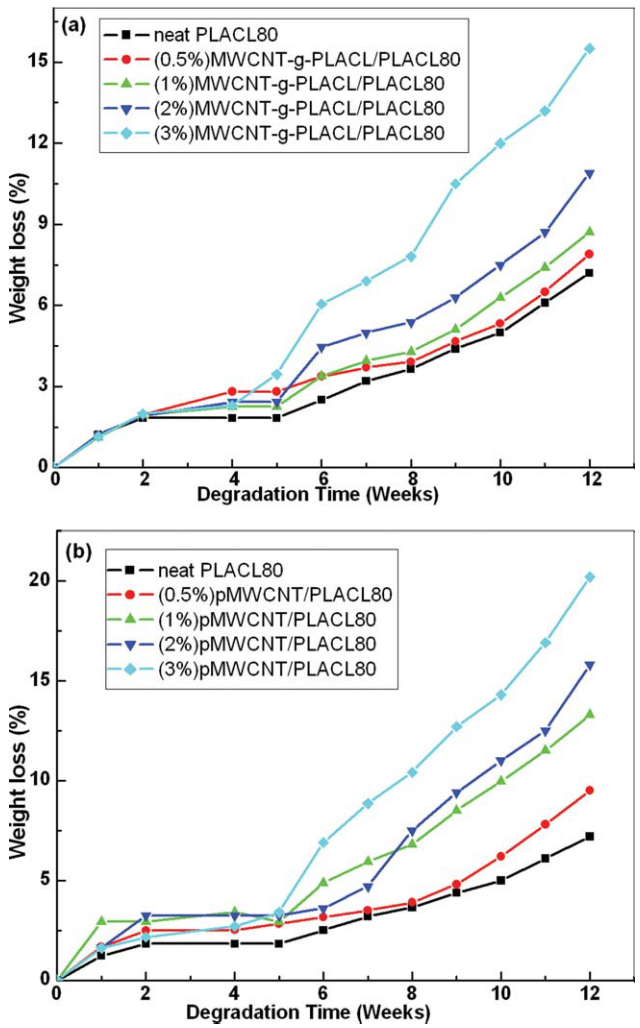

Figure 10 The weight loss of neat PLACL80 and its composites with MWCNT-*g*-PLACLs (a) and pMWCNTs (b) during degradation in PBS at 37°C and pH 7.4. [Color figure can be viewed in the online issue, which is available at wileyonlinelibrary.com.]

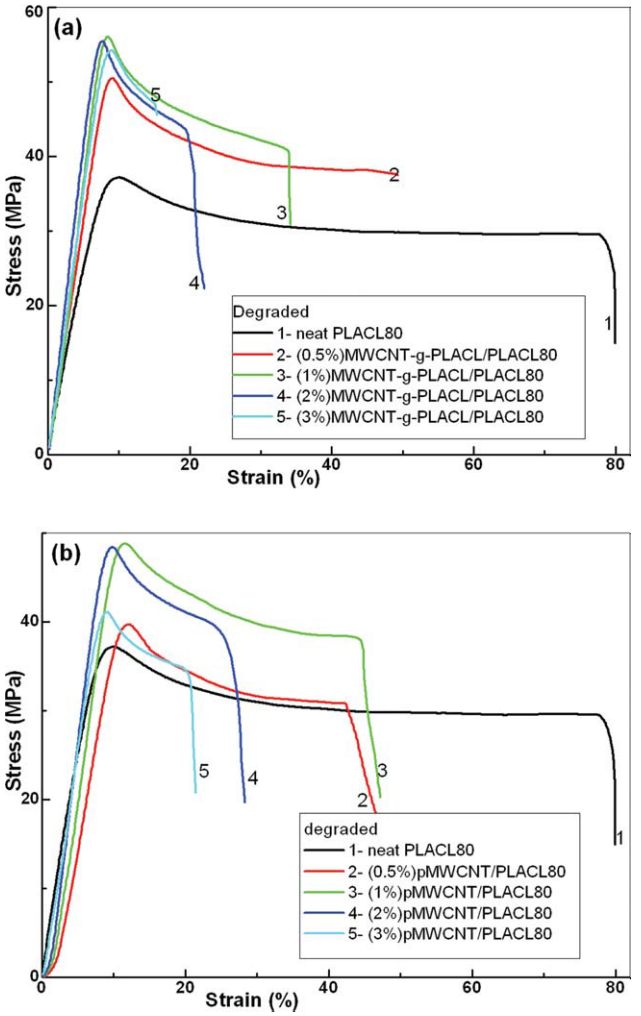

Figure 11 The stress versus strain curves of degraded neat PLACL80 and its composites with MWCNT-*g*-PLACLs (a) and pMWCNTs (b) after four weeks in PBS at 37°C and pH 7.4. [Color figure can be viewed in the online issue, which is available at wileyonlinelibrary.com.]

with MWCNTs was increased after degradation, while the melting point of degraded neat PLACL80 increased more than composites. The difference between the melting point of primary and degraded PLACL80 was decreased with increasing the contents of fillers. This effect is because of less increasing the crystallization of composites during degradation in presence of MWCNTs in comparison with neat PLACL80. The amorphous phase of components were degraded faster than crystalline phase. Hence, the ratio of crystalline phase on amorphous phase of polymer was increased during degradation. This effect indicates that the crystallinity of PLACL80 increased during degradation, and hence, the degraded PLACL80 was more rigid and brittle.

Figure 10 gives the weight loss of neat PLACL80 in comparison with its composites, with various concentrations of MWCNT-*g*-PLACLs and pMWCNTs after 12 weeks in PBS at 37°C. As can be seen, both

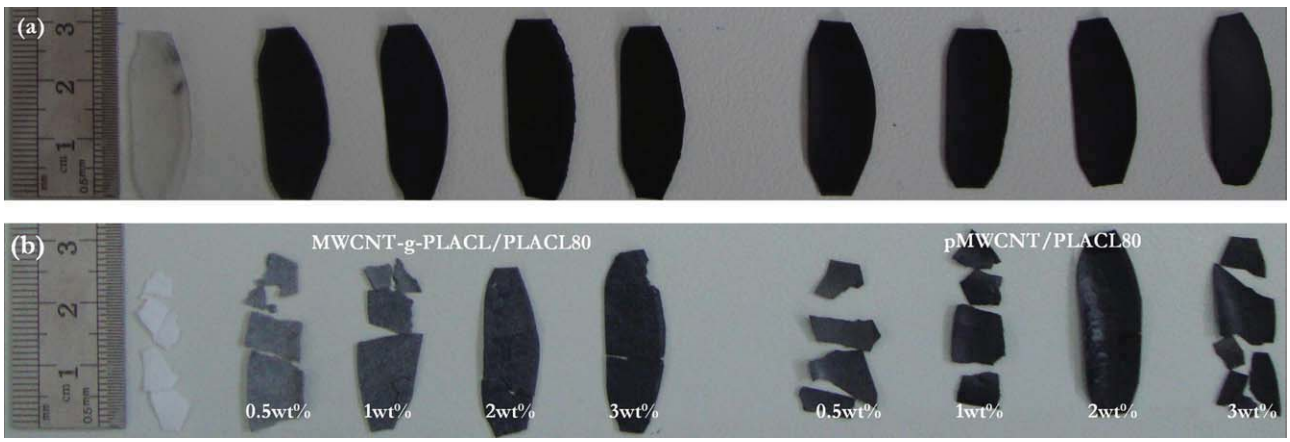

Figure 12 The photographs of neat PLACL80 and its composites with MWCNT-*g*-PLACLs and pMWCNTs before (a) and after six months (b) *in vitro* degradation in PBS at 37°C and pH 7.4. [Color figure can be viewed in the online issue, which is available at wileyonlinelibrary.com.]

kinds of MWCNTs increased the weight loss of PLACL80 during degradation. Because of diffusion of water from the surface of samples, the weight loss of all kinds of composites increases after four weeks. The increase in effective surface leads to increasing the hydrolysis rate. Thus, the degradation rate of samples increases with the increase of the degradation time. It can also be seen that the weight loss of the MWCNT-*g*-PLACL/PLACL80 and pMWCNT/PLACL80 composites increases with the filler contents increasing. There only exist the physical action between the MWCNTs and the PLACL80 copolymer matrix, which is benefit to the absorption of water and increase the weight loss. Moreover, pMWCNTs/PLACL80 are weaker than MWCNT-*g*-PLACL/PLACL80 against *in vitro* degradation in PBS.

Figure 11 presents the effect of *in vitro* degradation on mechanical properties of neat PLACL80 and its composites with various concentrations of pristine and functionalized MWCNTs. It is found that after four weeks degradation, the tensile modulus and yield stress of neat PLACL80 increased about 330% and 132%, respectively, while the elongation at break decreased about 68%. The mechanical properties of MWCNT/PLACL80 composites, such as neat PLACL80, were changed gradually. For degraded samples under tensile test, with increasing the loaded strain, this increase accompanied by an increase in the amount of strain softening, which takes place after yielding, while the primary samples only have stress increasing at strain increment. It should be noted that after longer time hydrolytic degradation, the samples become very brittle, and hence, it was difficult to determine the mechanical properties by tensile test [Fig. 12(a,b)].[33–35]

CONCLUSIONS

An alternative grafting from approach based on *in situ* ring opening polymerization of LA and CL has been developed to covalently graft biodegradable PLACL polymer chains from the surface of MWCNTs. This research suggests that the PLACL80 properties can be modified with introducing a small percentage of MWCNT-*g*-PLACLs. Surface functionalization of MWCNTs by carboxylation, hydroxylation, and polymer grafting appears to be effective in improving dispersion and their adhesion in PLACL80 matrix. The incorporation of MWCNT-*g*-PLACLs leads to much better reinforcing effect as compared with pMWCNTs. This suggests that improved dispersion and prevention of curling of MWCNTs are needed to fully realize the potential of MWCNTs in enhancing mechanical properties of PLACL biodegradable copolymers.

The presence of pristine or functionalized MWCNTs accelerated the hydrolytic degradation of the PLACL80 matrix and the weight loss of the nanocomposites. Another advantage of the CNTs is the promotion of a higher PLACL–water interaction. The degradation kinetics of nanocomposites for scaffolds can be engineered by varying the contents of CNTs. The combination of biodegradable polymers and CNTs opens in fact a new perspective in the self-assembly of nanomaterials and nanodevices for biomedical applications.[36,37]

References

1. Iijima, S. Nature 1991, 354, 56.
2. Bredeau, S.; Peeterbroeck, S.; Bonduel, D.; Alexandre, M.; Dubois, P. Polym Int 2002, 57, 547.
3. Coleman, J. N.; Khan, U.; Gunko, Y. K. Adv Mater 2006, 18, 689.
4. Ratna, D.; Karger-Kocsis, J. J Mater Sci 2008, 43, 254.
5. Moniruzzaman, M. I.; Winey, K. I. Macromolecules 2006, 39, 5194.
6. Coleman, J. N.; Cadek, M.; Blake, R.; Nikolosi, V.; Ryan, K. P.; Belton, C.; et al. Adv Funct Mater 2004, 14, 791.
7. Mitchell, C. A.; Krishnamoorti, R. Macromol 2007, 40, 1538.
8. Sun, L.; Warren, G. L.; O'Reilly, J. Y.; Everett, W. N.; Lee, S. M.; Davis, D.; Lagoudas, D.; Sue, H. J. Carbon 2008, 46, 320.

9. Zhang, D. H.; Kandadai, M. A.; Cech, J.; Roth, S.; Curran, S. A. J Phys Chem B 2006, 110, 12910.
10. Tsuji, H.; Kawashima, Y.; Takikawa, H.; Tanaka, S. Polymer 2007, 48, 4213.
11. Lu, X. L.; Cai, W.; Gao, Z. Y. J Appl Polym Sci 2008, 108, 1109.
12. Daniel, A. U.; Chang, M. K. O.; Andriano, K. P. J Appl Biomater 1990, 1, 57.
13. Pohjonen, T. P.; Helevirta, T. P.; Koskikare, K.; Pati, H.; Rokkanen, P. J Mater Sci Mater Med 1997, 8, 311.
14. Maquet, V.; Boccaccini, A. R.; Pravata, L.; Notingher, I. J Biomed Mater Res A 2003, 66, 335.
15. Bleach, N. C.; Nazhat, S. N.; Tanner, K. E.; Kellomaki, M. Biomaterials 2002, 23, 1579.
16. Kasuga, T.; Ota, Y.; Nogami, M.; Abe, Y. Biomaterials 2001, 22, 19.
17. Nishino, T.; Matsuda, H. I. K.; Nakamae, K. Polym Preprints Jpn 2003, 52, 4200.
18. Zhang, D.; Kandadai, M. A.; Cech, J.; Roth, S.; Seamus, A. J Phys Chem B 2006, 110, 12910.
19. Wu, D.; Wu, L.; Sun, Y.; Zhang, M. J Polym Sci: Part B: Polym Phys 2007, 45, 3137.
20. Wu, D.; Wu, L.; Zhang, M.; Zhao, Y. Polym Degrad Stab 2008, 93, 1577.
21. Wu, D.; Zhang, Y.; Zhang, M.; Yu, W. Biomacromol 2009, 10, 417.
22. Jana, R. N.; Cho, J. W. J Appl Polym Sci 2008, 110, 1550.
23. Chen, G. X.; Kim, H. S.; Park, B. H.; Yoon, J. S. Macromol Chem Phys 2007, 208, 389.
24. Kim, H. S.; Park, B. H.; Yoon, J. S.; Jin, H. J. Eur Polym Mater 2007, 43, 1729.
25. Saeed, K.; Park, S. Y.; Lee, H. J.; Baek, J. B.; Huh, W. S. Polymer 2006, 47, 8019.
26. Saeed, K.; Park, S. Y. J Appl Polym Sci 2007, 104, 1957.
27. Chen, G. X.; Shimizu, H. Polymer 2008, 49, 943.
28. Zeng, H. L.; Gao, C.; Yan, D. Y. Adv Funct Mater 2006, 16, 812.
29. Nabipour Chakoli, A.; Wan, J.; Feng, J. T.; Amirian, M.; Sui, J. H.; Cai, W. Appl Surf Sci 2009, 256, 170.
30. Yoon, J. T.; Lee, S. C.; Jeong, Y. G. Compos Sci Technol 2010, 70, 776.
31. Miyata, T.; Masuko, T. Polymer 1997, 38, 4003.
32. Pirlot, C.; Willems, I.; Fonseca, A.; Nagy, J. B.; Delhalle, J. Adv Eng Mater 2002, 4, 109.
33. Loh, X. J.; Colin Sng, K. B. C.; Li, J. Biomaterials 2008, 29, 3185.
34. Jeong, S. I.; Kim, B. S.; Kang, S. W.; Kwon, J. H.; Lee, Y. M.; Kim, S. H.; Kim, Y. H. Biomaterials 2004, 25, 5939.
35. Zhou, Z.; Yi, Q. F.; Liu, L.; Liu, X.; Liu, Q. J Macromol Sci Part B: Phys 2009, 48, 309.
36. Wick, P.; Manser, P.; Limbach, L. K.; Dettlaff-Weglikowska, U.; Krumeich, F.; Roth, S.; Stark, W. J.; Arie Bruinink, A. Toxicol Lett 2007, 168, 121.
37. Wei, W.; Sethuraman, A.; Jin, C.; Monteiro-Riviere, N. A.; Narayan, R. J. J Nanosci Nanotechnol 2007, 7, 1.